Equilibrium unfolding studies of the rat liver methionine adenosyltransferase III, a dimeric enzyme with intersubunit active sites

María GASSET*, Carlos ALFONSO†, José L. NEIRA‡, Germán RIVAS† and María A. PAJARES§[1]

*Instituto de Química-Física "Rocasolano" (CSIC), Serrano 119, 28006 Madrid, Spain, †Centro de Investigaciones Biológicas (CSIC), Velázquez 144, 28006 Madrid, Spain, ‡Centro de Biología Molecular y Celular, Universidad Miguel Hernández, Avda. del Ferrocarril s/n, 03202 Alicante, Spain, and §Instituto de Investigaciones Biomédicas "Alberto Sols" (CSIC), Arturo Duperier 4, 28029 Madrid, Spain

The reversible unfolding of rat liver methionine adenosyltransferase dimer by urea under equilibrium conditions has been monitored by fluorescence spectroscopy, CD, size-exclusion chromatography, analytical ultracentrifugation and enzyme activity measurements. The results obtained indicate that unfolding takes place through a three-state mechanism, involving an inactive monomeric intermediate. This intermediate has a 70% native secondary structure, binds less 8-anilinonaphthalene-1-sulphonic acid than the native dimer and has a sedimentation coefficient of 4.24 ± 0.15. The variations of free energy in the absence of denaturant [$\Delta G(H_2O)$] and its coefficients of urea dependence (m), calculated by the linear extrapolation model, were 36.15 ± 2.3 kJ·mol^{-1} and 19.87 ± 0.71 kJ·mol^{-1}·M^{-1} for the dissociation of the native dimer and 14.77 ± 1.63 kJ·mol^{-1} and 5.23 ± 0.21 kJ·mol^{-1}·M^{-1} for the unfolding of the monomeric intermediate respectively. Thus the global free energy change in the absence of denaturant and the m coefficient were calculated to be 65.69 kJ·mol^{-1} and 30.33 kJ·mol^{-1}·M^{-1} respectively. Analysis of the calculated thermodynamical parameters indicate the instability of the dimer in the presence of denaturant, and that the major exposure to the solvent is due to dimer dissociation. Finally, a minimum-folding mechanism for methionine adenosyltransferase III is established.

Key words: methionine metabolism, monomeric intermediate, *S*-adenosylmethionine.

INTRODUCTION

Methionine adenosyltransferases (MATs; EC 2.5.1.6) are a family of enzymes that catalyse the rate-limiting reaction in the methionine cycle, namely *S*-adenosylmethionine (AdoMet) synthesis [1]. These proteins are exceptionally well conserved during evolution [2], their sequence being detected even in the genome of *Mycoplasma genitalium*, considered to be the minimal set of genes needed for independent life [3,4]. MAT enzymes appear as homo-oligomeric proteins in all tissues and organisms studied to date, with the exception of mammalian MAT II [5]. All of them require Mg^{2+} ions and are activated by univalent cations (K^+). Most of them exhibit sigmoidal kinetics for their substrates and have tripolyphosphatase activity [5]. The importance of MAT enzymes is highlighted by the role of AdoMet as the major methyl donor in transmethylation reactions and as the source of propylamine moieties for the synthesis of polyamines [6]. Moreover, in mammalian liver, the transmethylation reactions, through the production of *S*-adenosylhomocysteine (AdoHcy), link AdoMet synthesis to the trans-sulphuration pathway and folate metabolism [7].

In mammals, two isoenzymes have been described, one ubiquitous (MAT II), and another whose expression is confined to the liver [5]. This latter protein appears in two oligomeric assemblies, a tetramer (MAT I) and a dimer (MAT III) that differ in their affinities for methionine, with the dimer having the lowest affinity for this substrate [5,8–10]. Moreover, MAT I is 10-fold more active than MAT III under physiological concentrations of methionine (60 μM) [8], a fact that has led to speculation about their cellular role [11]. Changes in the activity and oligomeric state have been described under pathological conditions [5]; in these cases the dimer becomes the prevalent form [12]. All of these findings have led to the study of the mechanisms controlling the MAT I/III exchange. In this context, Cys69Ser mutants have been shown to produce MAT only in a dimeric form, and site-directed mutagenesis of either of the cysteine residues found between positions 35 and 105 alters the MAT I/III ratio [13]. Other findings confirming the importance of cysteine residues on MAT have come from redox and nitrosylation experiments [9,14,15]. In redox experiments, inactivation and dissociation were observed [9,15], whereas during nitrosylation inactivation was detected when Cys-121 was modified [14]. Mutations in the MAT gene, generating truncated forms of 185 or 350–351 residues, have also been detected in patients with hypermethioninemia, but only the longer forms concurred with severe symptoms, such as demyelinization [16,17]. Moreover, a higher susceptibility to liver injury has been shown recently using knockout mice for this isoenzyme [18].

The structure of rat liver MAT has been determined by X-ray diffraction [19]. Each subunit of the protein (396 amino acids) [20] comprises three domains in the crystal structure; an N-terminal domain (residues 17–28 and 146–254); a central domain (residues 29–116 and 255–289); and a C-terminal domain (residues 129–145 and 290–396). A mobile loop links the central and the C-terminal domains. This loop, where Cys-121 is located, might regulate access to the active site by an open-to-closed conformational switch; an effect potentially due to nitrosylation [15]. The interaction between subunits in the dimer has been

Abbreviations used: AdoHcy, *S*-adenosylhomocysteine; AdoMet, *S*-adenosylmethionine; ANS, 8-anilinonaphthalene-1-sulphonic acid; ΔASA, accessible surface area; DTT, dithiothreitol; MAT, methionine adenosyltransferase.

[1] To whom correspondence should be addressed (e-mail mapajares@iib.uam.es).

described as a contact surface, which is mostly flat and hydrophobic between the β-sheets from each subunit. Comparison between the data of the two MAT structures available from *Escherichia coli* [21,22] and rat liver [19] show differences in the orientation of the subunits. The active site (two per dimer) has been located between the subunits, with amino acid residues from each monomer contributing to it. Moreover, the structural Mg^{2+} ions have been identified in co-ordination with the active-site residues that bind methionine [19]. Catalysis takes place in two steps; the synthesis of AdoMet produces tripolyphosphate as a product, and the resulting tripolyphosphate is hydrolysed to give pyrophosphate and P_i [1,23]. Several roles have been postulated for this tripolyphosphatase activity, including, among others, the prevention of the reversibility of the catalytic reaction and the production of the energy needed for a conformational change to accomplish the catalytic cycle [24].

The acquisition of structural data for rat liver MAT was only possible after heterologous overexpression and refolding from inclusion bodies free of the *E. coli* homologue [10,25]. This procedure revealed the dependence on Mg^{2+} ions for refolding, as well as an improved recovery if a two-step method through an intermediate concentration of denaturant was used. These findings raised the question of how a large multi-domain oligomeric protein with intersubunit active sites, such as MAT III, is folded. To date, there is a large body of work on the stability and thermodynamics of small monomeric proteins, but the number of studies on multimeric proteins, which, in most cases, do not exhibit reversible denaturation, is more limited [26,27]. In addition to intrachain interactions, oligomeric proteins show intersubunit interactions; the contribution of which to the energetics of the protein is not known. Equilibrium-unfolding studies could provide insights into the events occurring in the assembly of the individual chains. To address all of these questions, we have used a biophysical approach to investigate the equilibrium unfolding of MAT III by urea. The results obtained give the first stability data for this protein and allow a description of the minimum mechanism needed for the MAT dimer to fold.

EXPERIMENTAL

Materials

Dithiothreitol (DTT), protein standards for gel-filtration chromatography and 8-anilinonaphthalene-1-sulphonic acid (ANS) were purchased from Sigma Chemical Co. (St. Louis, MO, U.S.A.). YM-30 membranes and Microcon ultrafiltration products were purchased from Amicon (Millipore, Bedford, MA, U.S.A.). Biogel A 1.5 m and the bicinchoninic acid system were from Bio-Rad (Hercules, CA, U.S.A.) and Pierce (Rockford, IL, U.S.A.) respectively. Urea and buffers were from Merck (Darmstadt, Germany).

Expression and purification of recombinant rat liver MAT

Competent *E. coli* BL21 (DE3) cells were transformed with the plasmid pSSRL-T7N as described previously [10]. Cell growth, MAT expression and recovery of inclusion bodies were performed as described by López-Vara et al. [25]. Refolding of rat liver MAT III was then carried out in the presence of 10 mM DTT as described previously [25]. Refolded recombinant protein was fully characterized after purification and found to have identical behaviour and secondary structure to the MAT III purified from rat liver [25]. SDS/PAGE was performed on 10% gels under reducing conditions using the buffer system described previously to control the purity of the sample preparations [28]. When required, the protein was concentrated by ultrafiltration using either the Amicon cells or Microcon units with a YM-30 membrane. The protein concentration of the samples was measured spectrophotometrically using a calculated molar absorption coefficient (ϵ) at 280 nm of 41934 $M^{-1}\cdot cm^{-1}$ in 8 M urea.

MAT activity assay

MAT activity was measured using 0.02–0.05 mg/ml of protein essentially as described previously [29]. For the refolding measurements, MAT samples were denatured in the presence of 8 M urea for 2 h at 10 °C in buffer A [50 mM Tris/HCl (pH 8) and 75 mM $MgSO_4$] and then diluted with the same buffer to give the corresponding urea concentrations (8–0 M). The samples were then dialysed overnight at 4 °C in buffer A, and the activity was measured using the standard MAT reaction mixture (250 μl, final volume) as described previously [29]. For the unfolding measurements, MAT III samples were incubated in buffer A containing varying urea concentrations (0–8 M) for 2 h at 10 °C in a final volume of 160 μl prior to MAT activity determinations.

Unfolding and refolding experiments

The MAT III unfolding reactions were performed in buffer A containing varying concentrations of urea (0–8 M). Protein concentrations used were 0.08–0.02 mg/ml and 0.1–0.2 mg/ml for fluorescence and CD experiments respectively. Equilibrium was reached after a 2-h incubation period and experiments were performed after 12 h. Adding buffer to the unfolded samples and allowing each to re-equilibrate at lower urea concentrations established the reversibility of the process. The spectra acquired for these samples, when corrected for the dilution, were identical with those of the folded state, thus confirming the reversibility of the system.

Intrinsic fluorescence experiments

Urea-denatured and refolded samples were excited at 278 or 295 nm; the slit width was 2.5 nm for the excitation and 5 nm for the emission. The spectra of fluorescence intensity were recorded between 300 and 400 nm in a photon counting SLM-8000 spectrofluorimeter at 25 °C, using 0.5×0.5 cm cuvettes. The fluorescence signal for the protein was corrected by subtraction of the solvent signal.

ANS binding

A stock solution of ANS (1 mM) in methanol was prepared and its concentration was determined using $\epsilon = 6800\ M^{-1}\cdot cm^{-1}$ at 370 nm [30]. ANS was added to a pre-equilibrated unfolding reaction of MAT III (1 ml, 0.05 mg/ml) or to a control reaction without protein; the final methanol concentration in the sample was 0.04% (v/v). The study was performed using native, intermediate or unfolded states of MAT III at different ANS concentrations, or unfolding reactions of MAT III (0–8 M) and 40 μM ANS. The mixture was incubated for 1 h in the dark, and changes in ANS emission upon protein binding were monitored following the increase in the fluorescence emission at 470 nm from the spectra recorded between 400 and 600 nm, with excitation at 380 nm. Spectra were corrected for baseline and instrumental factors.

CD experiments

Far-UV CD spectra of urea-denatured or refolded MAT were recorded on a JASCO J-720 spectropolarimeter (Hachioji City,

Tokyo, Japan) at 25 °C [31], using samples with 0.1–0.2 mg/ml protein and 0.1 cm pathlength cuvettes. After baseline subtraction, the observed ellipticities were converted into mean residue ellipticities ($[\theta]_{m.r.w.}$) on the basis of a mean molecular mass per residue of 110 Da. Secondary-structure composition was calculated using the Convex Constraint Analysis (CCA) with the original set of reference proteins [32]. A minimum of five spectra were recorded for each sample.

Gel-filtration chromatography

MAT III samples (500 μl containing a minimum of 40 μg of protein), after incubation with 0–5 M urea, were loaded on to a Biogel A 1.5m gel-filtration column (50 cm × 1 cm). Equilibration and elution were performed using buffer A containing 50 mM KCl and the corresponding concentrations of urea at a flow rate of 15 ml/h in a 20 °C chamber. A_{280} was recorded and 500 μl fractions were collected and precipitated by trichloroacetic acid (10 %, v/v). The presence of protein after precipitation was determined using the bicinchoninic acid assay. The protein standards used were: Dextran Blue (2000 kDa), thyroglobulin (669 kDa), apoferritin (443 kDa), β-amylase (200 kDa), alcohol dehydrogenase (150 kDa) and carbonic anhydrase (29 kDa). For localization of the final volume, ATP (551 Da) was used. Under these conditions we found that the void volume (V_o, 15.5 ml) and total volume of the column (V_t, 37 ml) remained constant between 0 and 4 M urea.

Sedimentation velocity experiments

The experiments were performed at 188000 ***g*** and 18 °C in a Beckman Optima XL-A analytical ultracentrifuge (Beckman Instruments, Fullerton, CA, U.S.A.) equipped with absorbance optics, using an An50Ti rotor. Absorbance scans (0.005 cm step-size) were taken at 280 nm. Samples of urea-denatured MAT (0.1–0.2 mg/ml), prepared as above, were used in these experiments. The sedimentation velocity data were analysed with the program SVEDBERG [33]. Sedimentation velocity coefficients were corrected for solvent composition and temperature to obtain $s_{20,w}$ [34].

Analysis of the unfolding profiles

The unfolding profiles of MAT III by urea, monitored by its fluorescence intensity or its CD ellipticity, were analysed using Kaleidagraph (Synergy Software, Reading, PA, U.S.A.) and the equations described by Luo et al. [35] for a two- and a three-state model. No convergence of the data was observed using this procedure, and hence the data were analysed by clustering to three (native, unfolded and the transition between both states), five (native, intermediate I, native-intermediate I transition, unfolded and intermediate I-unfolded transition) or seven populations (native, intermediate I, native-intermediate I transition, intermediate J, intermediate I-intermediate J transition, unfolded and intermediate J-unfolded transition) using the SPSS program (SPSS, Chicago, IL, U.S.A.). These clusters allowed the calculation of estimates for the signals for Y_I, Y_J, $Y_N = y_N + m_N x$ and $Y_U = y_U + m_U x$ [where Y_U, Y_N, Y_I and Y_J are the signals from the CD or fluorescence analyses for the unfolded (U), native (N), intermediate I (I) and intermediate J (J) respectively; m_N and m_U, denaturant dependence for native and unfolded states; x, urea concentration; y_U and y_N, signals from the CD or fluorescence analyses for the unfolded (U) and native (N) states] and thus their use for free-energy determinations with the thermodynamic models described by Park and Bedouelle [36] for a two-state or a three-state mechanism. The equations for the four-state mechanism were developed in a similar way and are the following:

$$Y = Y_N(1-[K_2K_3+K_3+1]f_U)+2f_U(Y_IK_2K_3+Y_JK_3+Y_U)$$

$$f_I = K_2 f_J$$

$$f_J = K_3 f_U$$

$$f_N = 1-(K_2K_3+K_3+1)f_U$$

$$4cf_U{}^2+(K_2^3K_3^3+K_2^2K_3^3+K_2^2K_3^2)K_1f_U-K_1K_2^2K_3^2 = 0$$

$$K = K_1K_2^2K_3^2$$

$$\Delta G_1 = \Delta G_1(H_2O)-m_1x = -RT\ln(K_1)$$

$$\Delta G_2 = \Delta G_2(H_2O)-m_2x = -RT\ln(K_2)$$

$$\Delta G_3 = \Delta G_3(H_2O)-m_3x = -RT\ln(K_3)$$

$$\Delta G(H_2O) = \Delta G_1(H_2O)+2\,\Delta G_2(H_2O)+2\,\Delta G_3(H_2O)$$

The parameters are defined as: f_U, f_N, f_I and f_J, the fraction of protein in the unfolded, native and intermediate I and J states respectively; Y_I and Y_J are kept constant upon urea concentration; K_1, K_2 and K_3, the equilibrium constants for the N_2-2I, the 2I-2J and the 2I-2U transitions respectively; m_1, m_2 and m_3 the denaturant dependence for each transition; c, protein concentration; R, the gas constant; T, the absolute temperature; $\Delta G_1(H_2O)$, $\Delta G_2(H_2O)$ and $\Delta G_3(H_2O)$, the free energies for each transition in water; and $\Delta G(H_2O)$, the global free energy of the process.

RESULTS

Unfolding monitored by activity

Rat liver MAT III, the dimeric form of MAT, was used to characterize the unfolding reaction of the protein. The refolded MAT III used in these experiments is fully active and has been characterized previously to ensure that its behaviour is identical with the purified rat liver protein [25]. The ability to synthesize AdoMet was used to monitor the urea-induced unfolding of MAT III (Figure 1). MAT III activity decreased sharply with the addition of urea, with 50 % inactivation occurring at approx.

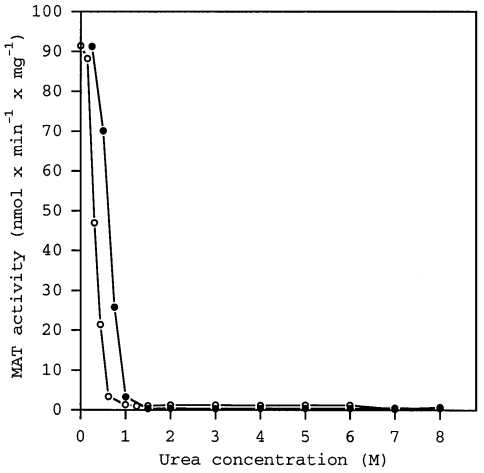

Figure 1 MAT III activity as a function of urea concentration

DTT-refolded MAT III (5 μg) was used for unfolding and refolding experiments. Unfolding was carried out by the addition of MAT to a solution containing different urea concentrations (0–8 M) in buffer A, and after a 2 h incubation MAT III activity was measured (○). Refolding was performed using MAT denatured in an 8 M urea solution in buffer A for 2 h. The denatured protein was then diluted to the corresponding urea concentrations (8–0 M), dialysed, and MAT activity was measured (●).

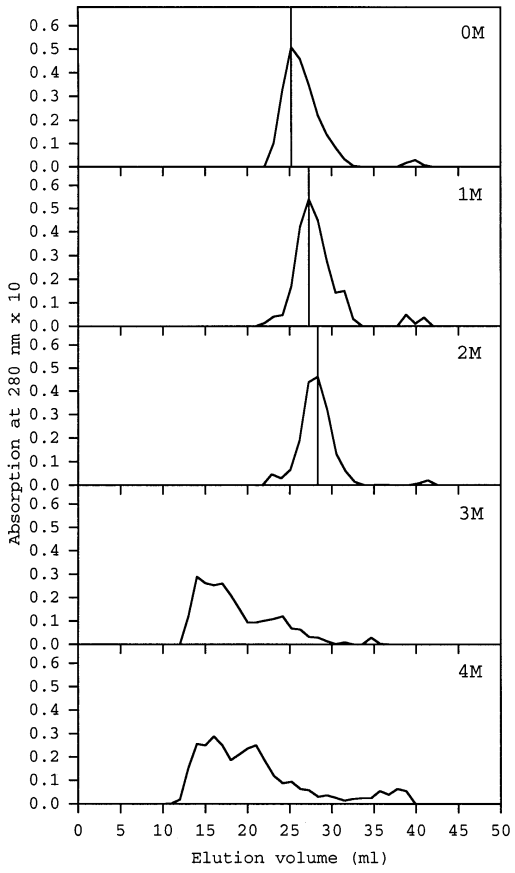

Figure 2 Unfolding of MAT III by urea monitored by gel-filtration chromatography

MAT III samples (0.2 mg/ml) were incubated with different concentrations of urea (0–4 M) for 2 h. Protein samples were then loaded on to a Biogel A 1.5 m column equilibrated in buffer A containing 50 mM KCl and the corresponding urea concentrations. Elution was followed by recording the A_{280}. The elution volumes of the protein standards were: Dextran Blue (15.5 ml), thyroglobulin (18.5 ml), apoferritin (21 ml), β-amylase (24 ml), alcohol dehydrogenase (25 ml) and carbonic anhydrase (32 ml). The urea concentration used in each case is indicated in the panel.

0.3 M urea. Removal of denaturant restored the initial activity, underlining the full reversibility of the process. This inactivation could be due to a local conformational change of MAT III, a weakening of the interactions between subunits where the active sites are located, or an effect of urea on the non-covalent interactions between the enzyme and its substrates or essential cations.

Molecular size changes of MAT III during unfolding

Thorough studies with monomeric proteins have shown that size-exclusion chromatography can be used to monitor the unfolding of proteins by denaturants, and to measure the molecular dimensions of their different conformational states [37]. With this technique, we observed that the protein was eluted as a single peak between 0 and 2 M urea, whereas, at higher denaturant concentrations, the protein profile was extended through all the chromatogram (Figure 2). In the presence of low urea concentrations (1–2 M), peak elution was delayed revealing an estimated molecular mass of 53000 Da, similar to that expected for a monomeric form. These data suggest the presence of a monomeric intermediate in MAT III unfolding.

Table 1 Comparison of the hydrodynamical parameters obtained by size-exclusion chromatography and analytical ultracentrifugation

MAT III samples were incubated in the presence of different urea concentrations until equilibrium was reached. These samples were then used for size-exclusion chromatography in the presence of the corresponding urea concentrations, and for sedimentation velocity experiments. The apparent molecular mass and Stokes radius values calculated from the gel filtration elution volumes and the calculated $s_{20,w}$ are shown for a representative experiment.

Urea concentration (M)	Molecular mass (kDa)	Stokes radius (nm)	$s_{20,w}$
0	108	3.9	5.4
1	59	2.9	4.56
2	53	2.7	4.24
3	—	—	3.81
4	—	—	3.53

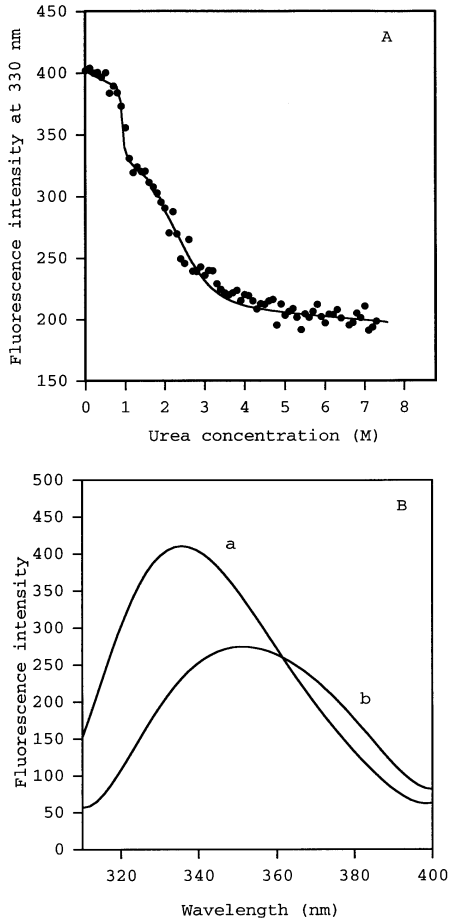

Figure 3 Unfolding of MAT III by urea as monitored by its fluorescence intensity

Purified MAT III samples (80 μg/ml) were used for unfolding studies in the presence of urea buffers. The emission of fluorescence at 330 nm was recorded after excitation of the samples at 295 nm. (**A**) Results from a typical experiment, with the solid line being the fitting of the data to the equations for an unfolding mechanism with a monomeric intermediate. (**B**) Fluorescence spectra for native dimeric MAT (line a) and the unfolded protein (line b).

To ensure that changes in the size of the MAT III molecule were obtained during urea denaturation, samples of the protein under different urea concentrations (0–8 M) were subjected to

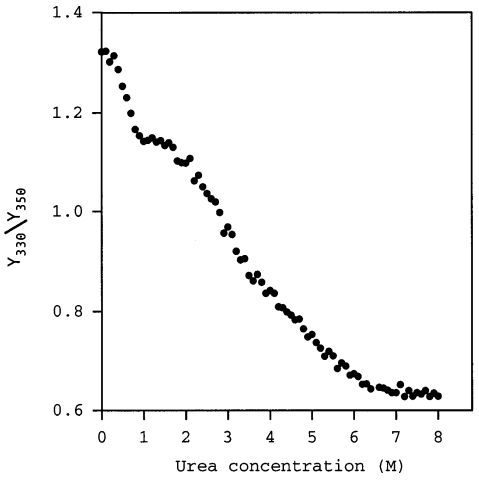

Figure 4 Unfolding of MAT III by urea, as monitored by the ratio of its fluorescence intensities at 330 and 350 nm (Y_{330}/Y_{350})

Y_{330} and Y_{350} are the corrected signals of fluorescence intensity upon excitation at 295 nm. The concentration of protein in the experiment was 80 μg/ml. The calculated ratio for a typical experiment is shown.

analytical ultracentrifugation experiments. Sedimentation equilibrium and overspeeding experiments render confusing results, due to the instability of the protein under those conditions (results not shown), and hence sedimentation velocity was used. Under these conditions, it was possible to observe a decrease in the calculated $s_{20,w}$ in the presence of denaturant (Table 1). Again, in the presence of low concentrations of urea (1–2 M), the values calculated corresponded to a monomeric MAT. These data, together with those of the size-exclusion chromatography, indicated that urea unfolding of MAT III takes place through a monomeric intermediate.

Unfolding monitored by fluorescence spectroscopy

Rat liver MAT III contains 13 tyrosine and four tryptophan residues (at positions 176, 275, 301 and 388). According to its crystal structure [19], several of these intrinsic fluorophores, in particular the tryptophan residues, have their side chains buried inside the protein subunit. We have recorded fluorescence emission spectra of MAT III in 0–8 M urea at excitation wavelengths of 278 or 295 nm. Native MAT III emission is maximal at 334 nm at both excitation wavelengths, whereas the spectrum of unfolded MAT is red-shifted to 350 nm, as expected for solvent-exposed tryptophan (Figure 3). This shift was accompanied by a decrease in intensity (Figure 3B). As expected, the difference in fluorescence intensity was larger when the excitation wavelength was 278 nm than at 295 nm, since both tyrosine and tryptophan residues are excited at 278 nm, whereas only tryptophan is excited at 295 nm. This difference between the native and unfolded states of MAT III was maximal at an emission wavelength of approx. 330 nm. Therefore the intensity of fluorescence emission at 330 nm was used to monitor the unfolding of MAT III by urea under equilibrium conditions using several protein concentrations (Figure 3A). In each case, fluorescence intensity started to decay as soon as the denaturant was added, decreased non-linearly between 2 and 5 M urea, and then remained approximately constant at higher denaturant concentrations. Refolding of the protein produced superimposable

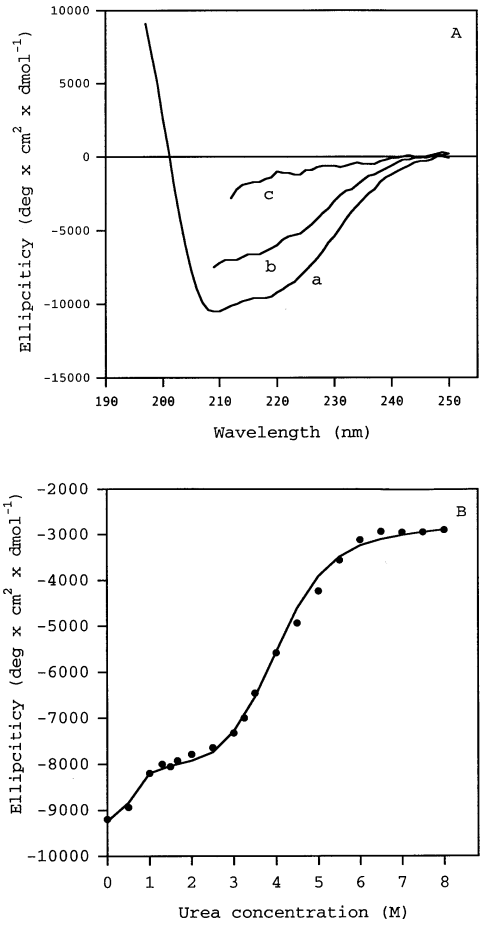

Figure 5 Unfolding of MAT III by urea monitored by its CD ellipticity

Samples of 0.2 mg/ml of DTT-refolded MAT III were incubated with different concentrations of urea (0–8 M) in buffer A. (**A**) The mean of five independent spectra for native MAT III (curve a), intermediate at 1.5 M urea (curve b), and denatured at 8 M urea (curve c). (**B**) The CD ellipticity at 220 nm as a function of urea concentration. The corrected signal for a typical experiment is given along the y-axis; the solid line is the fitting of the data to the equations for an unfolding mechanism with a monomeric intermediate.

fluorescence data (results not shown). This biphasic profile suggested a two-state unfolding model.

To get an insight into the average exposure of the tryptophan residues during unfolding, the ratio of fluorescence intensities at 330 and 350 nm (Y_{330}/Y_{350}) was studied as a function of urea concentration (Figure 4). The profiles obtained were similar to those of fluorescence intensity, but in this case values between 1 and 2 M urea remained almost constant, suggesting the possible presence of an intermediate state during unfolding.

Unfolding monitored by CD

We used the CD of MAT III in the absorption band of the peptide bond (from 200–230 nm) to monitor the variation in its secondary-structure content during urea unfolding (Figure 5). For sensitivity reasons, the protein concentrations used in the CD experiments were higher than those for fluorescence experiments. As previously reported [25], a minimum at 222 nm and a shoulder at 210 nm are features of the native MAT III spectrum (Figure 5A; curve a). Spectral deconvolution using the Convex Constraint Analysis showed that the major secondary element was the β-sheet, in agreement with the crystallographic data [19].

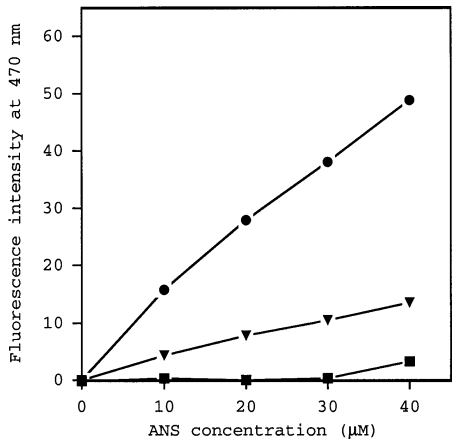

Figure 6 ANS binding to MAT III under different unfolding conditions

MAT III (50 μg/ml) was incubated in the presence of 0, 2 and 8 M urea to obtain the native (●), intermediate (▼) and unfolded (■) states of the protein respectively. Once the equilibrium was reached, different concentrations of ANS were added to the samples for 1 h in the dark. ANS binding was measured by fluorescence intensity at 470 nm using an excitation wavelength of 380 nm.

In the presence of 8 M urea, the CD spectra resembled that of an unfolded protein (Figure 5A; curve c). Ellipticity plots at 220 nm, as a function of urea concentration, revealed a sharp increase up to a plateau between 1 and 2.5 M, followed by an additional increase up to 6 M urea (Figure 5B). Refolding profiles showed an identical behaviour (results not shown). Again the profile obtained seemed to indicate the possible presence of an intermediate form in the unfolding process. In the light of these results, the first transition could be attributable to changes due to dimer dissociation, whereas the changes observed at higher urea concentrations may arise from monomer denaturation.

ANS binding

ANS is a hydrophobic dye that fluoresces in apolar solvents, but little in water. Some proteins unfold through a conformational intermediate state that binds ANS more than the native state, thus indicating a change that increases its apolar surface [38]. We have measured ANS binding to MAT III in the presence of urea under equilibrium conditions using a minimum of a 10-fold molar excess of the fluorescent probe over the calculated protein concentration and an excitation wavelength of 380 nm (Figure 6). The results obtained indicated that the intermediate state observed at 2 M urea binds ANS, but to a lesser extent than the MAT III native state. For a given concentration, the intermediate ANS binding is approx. 25% of that exhibited by the native dimer. Data showing the dependence of ANS binding upon denaturant concentration were also obtained, but were not clear enough to yield precise thermodynamic parameters (results not shown).

Characteristic parameters of unfolding monitored by fluorescence intensity and CD

Fluorescence profiles obtained from MAT III unfolding experiments, assuming a linear relationship with the denaturant concentration (x), made the determination of the fluorescence intensity of the native state ($Y_N = y_N + m_N x$) difficult. Hence, after the failure of other approaches, a clustering analysis of the data was performed to determine Y_N. The values included in the clusters were also used to determine the fluorescence intensity of the unfolded state ($Y_U = y_U + m_U x$) and possible intermediate states (Y_I, Y_J), with a linear relationship and a constant fluorescence with urea concentration respectively. The calculated Y_N, Y_U and Y_I values were used to fit equation 13 described by Park and Bedouelle [36] and, in addition to Y_J, to fit the four-state model equations described in the Experimental section of the present study. These equations link the observed fluorescence intensity and the urea concentration with the unfolding profiles for the following mechanisms: a two-state model; a three-state model with a monomeric intermediate; or a four-state model with two different monomeric intermediates. The $\Delta G(H_2O)$ and m values for the models were obtained using the linear extrapolation model, except for the four-state model that did not fit to our experimental data (Table 2). The thermodynamic parameters (equilibrium constants and associated free energies) corresponding to these fittings remained constant within the experimental error when the protein concentration was changed (results not shown). Since all the experimental results indicated the presence of a monomeric intermediate and no fitting was obtained for a four-state model, the three-state model was selected for further calculations.

Using the data obtained in the CD experiments, good fits were only possible with the three-state model. In this case, the values calculated for the thermodynamical parameters were similar to those obtained from the fluorescence intensity profiles (Table 2). In the CD experiments, m_2 was calculated to be slightly lower (3.97 ± 0.08 kJ·mol^{-1}·M^{-1}) than the corresponding fluorescence value.

We obtained the molar fractions, f_N, f_I and f_U, of the different conformational states of MAT III from the thermodynamic parameters for an unfolding mechanism with a monomeric

Table 2 Comparison of the thermodynamical parameters of different mechanism for the unfolding of MAT III

Unfolding of MAT III by urea was monitored by fluorescence intensity as described in the Experimental section. The thermodynamic parameters $\Delta G(H_2O)$ and m were obtained by fitting the experimental data to the equations described by Park and Bedouelle [36] for the three-state model with a monomeric intermediate (with monomeric intermediate) and a coupled two-state unfolded-dissociation model (without intermediate state). Results represent the global average parameter ± S.D. obtained from three independent experiments carried out at three different protein concentrations.

	Thermodynamic parameters					
	$\Delta G(H_2O)$ (kJ·mol^{-1})			m (kJ·mol^{-1}·M^{-1})		
Model	$\Delta G(H_2O)$	$\Delta G_1(H_2O)$	$\Delta G_2(H_2O)$	m	m_1	m_2
Without intermediate state	41.25 ± 1.76			3.18 ± 0.33		
With monomeric intermediate		36.15 ± 2.3	14.77 ± 1.63		19.87 ± 0.71	5.23 ± 0.211

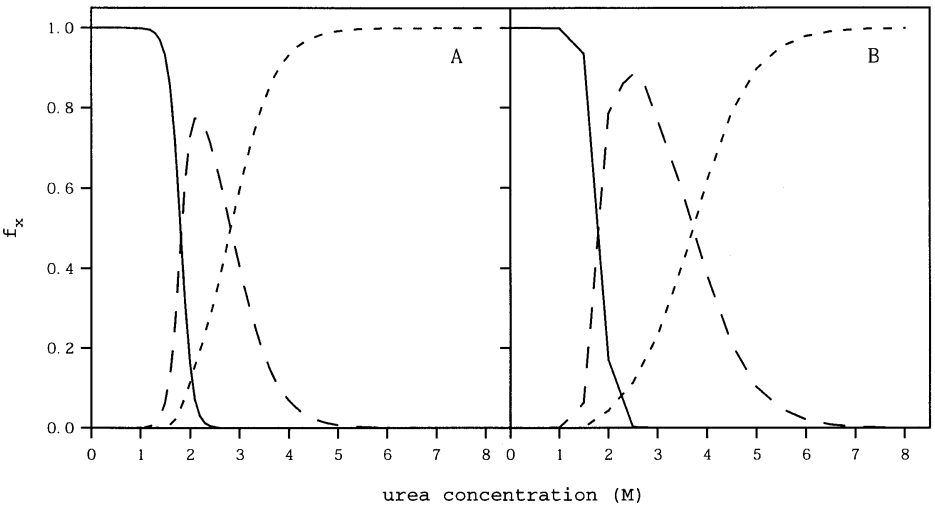

Figure 7 Fraction of each MAT state during unfolding with urea

The fractions, f_N, f_I and f_U, of MAT in the native (—), monomeric intermediate (– – –) and unfolded (- - - -) states respectively, were calculated from the experimental data obtained by fluorescence spectroscopy (using 80 μg/ml MAT) (**A**) and CD (using 0.2 mg/ml MAT) (**B**). The average thermodynamical parameters used for these calculations were those shown in Table 2, except for the m_2 value for CD, which was 3.97 kJ·mol^{-1}·M^{-1}.

Table 3 Characteristic concentrations of urea for the unfolding of MAT III as monitored by its fluorescence intensity and CD ellipticity

The characteristic concentrations of urea were calculated using the thermodynamical parameters listed in Table 2 and equations 10–12 from Park and Bedouelle [36]. Results are means ± S.D. of three independent experiments carried out using 80 μg/ml MAT for fluorescence intensity and 0.1 mg/ml MAT for CD. Abbreviations used: f_I^{-1}(max f_I) the concentration at which the monomeric intermediate was maximal; f_N^{-1} (0.5) the concentration at which half of the MAT III molecules were dissociated; f_U^{-1}(0.5) the concentration at which half of the molecules were unfolded.

	Characteristic concentrations of urea (M) required for unfolding		
Experimental procedure	f_I^{-1}(max f_I)	f_N^{-1} (0.5)	f_U^{-1}(0.5)
Fluorescence intensity	2.20 ± 0.05	1.82 ± 0.06	2.85 ± 0.06
CD	2.50 ± 0.10	1.70 ± 0.25	3.75 ± 0.08

intermediate (Figure 7). Several characteristic concentrations of urea can be deduced from these molar fractions: f_I^{-1}(max f_I), the concentration at which the monomeric intermediate was maximal; f_N^{-1}(0.5), the concentration at which half of the MAT III molecules were dissociated; and f_U^{-1}(0.5), the concentration at which half of the molecules were unfolded. The calculated values for the fluorescence intensity and CD experiments are shown in Table 3. The f_U^{-1}(0.5) values for both techniques were calculated on the basis of the m_2 values obtained and thus are different.

The global average values of the four thermodynamic parameters that characterized the unfolding reaction were calculated from the experiments performed at different protein concentrations (Table 2), namely, the free energy of dissociation of the native MAT III [$\Delta G_1(H_2O)$] and the free energy of the unfolding of the monomeric intermediate in the absence of urea [$\Delta G_2(H_2O)$], and their corresponding coefficients of dependence on the concentration of urea (m_1 and m_2 respectively). The values of the total parameters, $\Delta G(H_2O)$ and m, calculated by the equations described by Park and Bedouelle [36] for a three-state model with a monomeric intermediate, were determined to be 65.69 kJ·mol^{-1} and 30.33 kJ·mol^{-1}·M^{-1} respectively.

DISCUSSION

MAT III is the dimeric form of liver-specific MAT [8,39] and has been used under several experimental conditions to monitor unfolding by urea. The measurements were carried out after a minimum of 2 h when equilibrium conditions were reached. Unfolding of MAT III is reversible, as shown by the agreement of the unfolding and refolding profiles obtained by spectrofluorimetry, CD and activity experiments. Independent of the protein concentrations tested (0.02–0.2 mg/ml) and the technique used (fluorescence spectroscopy, CD, analytical ultracentrifuge, gel-filtration chromatography and ANS binding), our results indicate that the MAT dimer unfolds following a three-state mechanism through a monomeric intermediate. The absence of the concentration dependency observed in the N-I transition could be due to the low protein concentrations used in our experiments, and thus dissociation greatly favoured the monomer conformation even at low denaturant concentrations. Moreover, similar values for the total free energy of unfolding under the different experimental conditions tested were obtained. The low value of $\Delta G(H_2O)$ (65.69 kJ·mol^{-1}) is an indicator of the instability of the dimer, as compared with that obtained for dimeric proteins of thermophilic origin [36]. This is probably due to the low value of $\Delta G_1(H_2O)$ determined for the dissociation and unfolding of the dimer (36.14 ± 2.3 kJ·mol^{-1}), plus an even lower value of $\Delta G_2(H_2O)$ (14.77 ± 1.63 kJ·mol^{-1}) for the unfolding of the monomeric intermediate. The $\Delta G_2(H_2O)$ value is approximately one-quarter of the calculated free energy of unfolding of soluble globular monomeric proteins in the presence of denaturant, calculated by Privalov [40] to be approx. 48.12 kJ·mol^{-1} (11.5 kcal·mol^{-1}). From these values, it can be deduced that approximately half of the global energy of stabilization for MAT III comes from the association between both subunits, and one-quarter from the secondary and tertiary interactions stabilizing each of the monomeric intermediates. These data suggest that quaternary association is a key element in the stabilization of the multimeric assembly, as has been shown in other multimeric proteins [26,27,36,41–44]. However, it must be emphasized that all of these results were obtained using the linear extrapolation

model and have to be considered under the limitations of such method.

Myers et al. [45] suggested that the denaturant m value and the number of residues in a protein are strongly correlated with the variation of accessible surface area (ΔASA). In spite of the uncertainties in the theoretical findings, it would be interesting to analyse our experimental results in the light of these observations. Thus the relationship between m and ΔASA can be used with dimeric MAT and its monomeric intermediate to calculate the values of m and m_2. For this purpose, ΔASA for both the native dimer (72749 Å^2; where 1 Å = 0.1 nm) and monomeric intermediate (35921 Å^2) can be calculated using the number of residues for both forms of the protein, 792 and 396 respectively. The predicted and measured values of m (34.6 and 30.33 kJ·mol^{-1}·M^{-1} respectively) were in reasonable agreement according to the limitations of the data used for these calculations (size of the protein, oligomeric state and unfolding mechanism). As for m_2, comparison of the predicted and experimental values (17.99 and 5.23 ± 0.21 kJ·mol^{-1}·M^{-1} respectively) showed that unfolding of the monomeric intermediate increased solvent exposure by only one-third of what was expected theoretically. The 70 % difference observed between the predicted and measured values could be due, among other factors, to a larger accessible surface area than that for native monomeric proteins of a similar size. Furthermore, the hydrophobic core of MAT III was partially exposed to the solvent in the intermediate state, but to a lesser extent than in the native protein, as suggested by the ANS measurements. ANS binding of native proteins has been observed in other oligomers [46], but it is uncommon that the surface exposed to the dye is larger in the oligomer than the intermediate state. However, this behaviour of the native dimer in the presence of ANS may be expected, as previous findings [47,48] have demonstrated that MAT III binds strongly to hydrophobic chromatography media, a characteristic that is exploited during its purification. Another possibility to explain the larger fluorescence intensity observed in the native MAT III may be due to the influence of the environmental polarity of the binding site, which may differ from the dimeric to the intermediate state [49]. On the other hand, the calculated m_1 value for the dissociation and unfolding of the dimer shows even larger deviations from the predicted value (19.87 and -1.38 kJ·mol^{-1} M^{-1} respectively), indicating a much larger exposure to the solvent. Similar m values have been described for other multimeric proteins, such as p53 [42], thus indicating deviations from theoretical and experimental determinations in oligomers. All these discrepancies can be explained by the crystal structure of MAT [19], where monomers have a large hydrophobic surface of contact and hence, dissociation would expose it to the solvent. The different ANS properties of the intermediate and native dimer probably suggest a rearrangement of the individual monomer chain, which causes burial of the hydrophobic surface upon monomer formation, leading to a high m_1 value. Thus only minimal changes would be required for the monomeric intermediate to produce the unfolded state.

Unfolding of MAT III by urea was monitored using several techniques. The intensity of fluorescence at 330 nm allowed the identification of multiple equilibria in the presence of denaturant among the native dimeric state, a monomeric intermediate and the unfolded state. The monomeric intermediate was calculated to have a 2.5-fold lower fluorescence intensity than the native MAT III. This variation of intensity could be due to global or local structural changes around some of the intrinsic fluorophores (tryptophan and tyrosine residues), or to the loss of fluorescence transfer between tyrosine and tryptophan residues of both subunits upon dissociation. The ratio of fluorescence intensities at 330 and 350 nm indicated that the environment of the tryptophan residues became more solvent-exposed in both native-intermediate I and intermediate I-unfolded transitions. The Y_{330}/Y_{350} data seem to indicate that, in both the native and the intermediate states, the tryptophan residues were partially buried, probably being deeply located in the intermediate states, since the change is larger in the intermediate I-unfolded transition. According to the CD ellipticity, this intermediate possessed a large part (70 %) of the secondary structure of the native MAT III, as has been observed in the intermediate states of other proteins that follow non-two-state unfolding processes [50]. In addition, the ANS-binding data indicated that this intermediate was more compact than the native state. However, the CD data may be influenced by the presence of aromatic residues that could change their environment upon intermediate formation [51]. Thus these results indicate that the intermediate state detected exhibits some of the characteristics of a molten globular state, but has undergone certain structural rearrangements to prevent maximal hydrophobic surface exposure.

Finally, the activity of AdoMet synthesis showed that total inactivation of MAT III was obtained at 1 M urea, when, as calculated from the results of fluorescence and CD experiments, 99 % of MAT III is still dimeric. These results differed from those of the size-exclusion chromatography and analytical ultracentrifugation experiments, where, at this denaturant concentration, the presence of monomeric protein was already detectable. Together, these data indicated that, as the urea concentration increased, the MAT dimer was inactivated either slightly before or upon dissociation into monomers. Such a conclusion coincided with what can be expected from the structure [19] where active sites are located between subunits, with amino acids of both monomers contributing to them. Moreover, loosening of subunit interactions may produce Mg^{2+} loss before dissociation; a fact shown in refolding experiments that would lead to inactivation. In addition, the area of contact between subunits is defined as ''mostly flat and hydrophobic'' and formed mainly by β-sheets [19]. Therefore this dissociation will lead to the exposure of a large hydrophobic surface to the media. Hence it may be expected that the domain organization is altered when compared with the subunit in the dimer, since the dissociated monomer preserves most of the secondary structure content of the native MAT III. The importance of a monomeric intermediate prior to oligomerization is more apparent in the case of long-truncated MAT forms (350–351 amino acids long), such as those detected in hypermethioninemic patients [16,17]. These truncated MATs lack part of the C-terminal domain of the protein, but, as deduced from the crystallographic data [19], contain the residues involved in subunit–subunit interactions. Therefore it could be possible that these truncated forms fold to give a monomeric intermediate, which is capable of interacting with the complete subunit intermediate. This heterodimer would capture the normal MAT subunits, leading to the important reduction in MAT activity detected in these patients.

In summary, the findings presented in this study suggest that urea-induced unfolding of MAT III can be better explained according to a three-state mechanism through a monomeric intermediate, and are the first estimation of the thermodynamic parameters for MAT III dissociation.

We thank F. Garrido for technical assistance.

REFERENCES

1 Cantoni, G. L. (1953) *S*-adenosylmethionine: a new intermediate formed enzymatically from L-methionine and adenosine triphosphate. J. Biol. Chem. **204**, 403–416

2 Kotb, M. and Geller, A. M. (1993) Methionine adenosyltransferase: structure and function. Pharmacol. Ther **59**, 125–143
3 Fraser, C. M., Gocayne, J. D., White, O., Adams, M. D., Clayton, R. A., Fleischmann, R. D., Bult, C. J., Kerlavage, A. R., Sutton, G., Kelley, J. M. et al. (1995) The minimal gene complement of *Mycoplasma genitalium*. Science (Washington, D.C.) **270**, 397–403
4 Bult, C. J., White, O., Olsen, G. J., Zhou, L., Fleischmann, R. D., Sutton, G. G., Blake, J. A., FitzGerald, L. M., Clayton, R. A., Gocayne, J. D. et al. (1996) Complete genome sequence of the methanogenic archaeon, *Methanococcus jannaschii*. Science (Washington, D.C.) **273**, 1058–1073
5 Mato, J. M., Alvarez, L., Ortiz, P. and Pajares, M. A. (1997) *S*-adenosylmethionine synthesis: molecular mechanisms and clinical implications. Pharmacol. Ther. **73**, 265–280
6 Cantoni, G. L. (1975) Biochemical methylations: selected aspects. Annu. Rev. Biochem. **44**, 435–441
7 Finkelstein, J. D. and Mudd, S. H. (1967) Transsulfuration in mammals: the methionine sparing effect of cystine. J. Biol. Chem. **242**, 873–880
8 Cabrero, C., Puerta, J. L. and Alemany, S. (1987) Purification and comparison of two forms of *S*-adenosyl-L-methionine synthetase from rat liver. Eur. J. Biochem. **170**, 299–304
9 Pajares, M. A., Durán, C., Corrales, F., Pliego, M. M. and Mato, J. M. (1992) Modulation of rat liver *S*-adenosylmethionine synthetase activity by glutathione. J. Biol. Chem **267**, 17598–17605
10 Alvarez, L., Mingorance, J., Pajares, M. A. and Mato, J. M. (1994) Expression of rat liver *S*-adenosylmethionine synthetase in *Escherichia coli* results in two active oligomeric forms. Biochem. J. **301**, 557–561
11 Martinov, M. V., Vitvitsky, V. M., Mosharov, E. V., Banerjee, R. and Ataullakhanov, F. I. (2000) A substrate switch: a new mode of regulation in the methionine metabolic pathway. J. Theor. Biol. **204**, 521–532
12 Cabrero, C., Martín-Duce, A., Ortíz, P., Alemany, S. and and Mato, J. M. (1988) Specific loss of the high-molecular weight form of *S*-adenosyl-L-methionine synthetase in human liver cirrhosis. Hepatology (Philadelphia) **8**, 1530–1534
13 Mingorance, J., Alvarez, L., Sánchez-Góngora, E., Mato, J. M. and Pajares, M. A. (1996) Site-directed mutagenesis of rat liver *S*-adenosylmethionine synthetase. Identification of a cysteine residue critical for the oligomeric state. Biochem. J. **315**, 761–766
14 Avila, M. A., Mingorance, J., Martínez-Chantar, M. L., Casado, M., Martín-Sanz, P., Boscá, L. and Mato, J. M. (1997) Regulation of rat liver *S*-adenosylmethionine synthetase during septic shock: role of nitric oxide. Hepatology (Philadelphia) **25**, 391–396
15 Sánchez-Góngora, E., Ruiz, F., Mingorance, J., An, W., Corrales, F. J. and Mato, J. M. (1997) Interaction of rat liver methionine adenosyltransferase with hydroxyl radical. FASEB J. **11**, 1013–1019
16 Chamberlin, M. E., Ubagai, T., Mudd, S. H., Wilson, W. G., Leonard, J. V. and Chou, J. Y. (1996) Demyelination of the brain is associated with methionine adenosyltransferase I/III deficiency. J. Clin. Invest. **98**, 1021–1027
17 Hazelwood, S., Bernardini, I., Shotelersuk, V., Tangerman, A., Guo, J., Mudd, H. and Gahl, W. A. (1998) Normal brain myelination in a patient homozygous for a mutation that encodes a severely truncated methionine adenosyltransferase I/III. Am. J. Med. Genet. **75**, 395–400
18 Lu, S. C., Alvarez, L., Huang, Z. Z., Chen, L., An, W., Corrales, F. J., Avila, M. A., Kanel, G. and Mato, J. M. (2001) Methionine adenosyltransferase 1A knockout mice are predisposed to liver injury and exhibit increased expression of genes involved in proliferation. Proc. Natl. Acad. Sci. U.S.A. **98**, 5560–5565
19 González, B., Pajares, M. A., Hermoso, J., Alvarez, L., Garrido, F., Sufrin, J. R. and Sanz-Aparicio, J. (2000) The crystal structure of tetrameric methionine adenosyltransferase from rat liver reveals the methionine-binding site. J. Mol. Biol. **300**, 363–375
20 Horikawa, S., Ishikawa, M., Ozasa, H. and Tsukada, K. (1989) Isolation of a cDNA encoding the rat liver *S*-adenosylmethionine synthetase. Eur. J. Biochem. **184**, 497–501
21 Takusagawa, F., Kamitori, S. and Markham, G. D. (1996) Structure and function of *S*-adenosylmethionine synthetase: crystal structures of S-adenosylmethionine synthetase with ADP, BrADP and PP_i at 2.8 Å resolution. Biochemistry **35**, 2586–2596
22 Takusagawa, F., Kamitori, S., Misaki, S. and Markham, G. D. (1996) Crystal structure of *S*-adenosylmethionine synthetase. J. Biol. Chem. **271**, 136–147
23 McQueney, M. S. and Markham, G. D. (1995) Investigation of monovalent cation activation of *S*-adenosylmethionine synthetase using mutagenesis and uranyl inhibition. J. Biol. Chem. **270**, 18277–18284
24 Reczkowski, R. S., Taylor, J. C. and Markham, G. D. (1998) The active-site arginine of *S*-adenosylmethionine synthetase orients the reaction intermediate. Biochemistry **37**, 13499–13506
25 López-Vara, M. C., Gasset, M. and Pajares, M. A. (2000) Refolding and characterization of rat liver methionine adenosyltransferase from *Escherichia coli* inclusion bodies. Protein Expression Purif. **19**, 219–226
26 Robinson, C. R., Rentzeperis, D., Silva, J. L. and Sauer, R. T. (1997) Formation of a denatured dimer limits the thermal stability of Arc repressor. J. Mol. Biol. **273**, 692–700
27 Jaenicke, R. and Lilie, H. (2000) Folding and association of oligomeric and multimeric proteins. Adv. Protein Chem. **53**, 329–401
28 Laemmli, U.K. (1970) Cleavage of structural proteins during the assembly of the head of bacteriophage T4. Nature (London) **227**, 680–685
29 Gil, B., Pajares, M. A., Mato, J. M. and Alvarez, L. (1997) Glucocorticoid regulation of hepatic *S*-adenosylmethionine synthetase gene expression. Endocrinology **138**, 1251–1258
30 Haugland, R. P. (1991) Handbook of Fluorescent Probes and Research Chemicals, Molecular Probes, Eugene, OR
31 Medrano, F. J., Gasset, M., López-Zumel, C., Usobiaga, P., García, J. L. and Menéndez, M. (1996) Structural characterization of the unligated and choline-bound forms of the major pneumococcal autolysin LytA amidase: conformational transitions induced by temperature. J. Biol. Chem. **271**, 29152–29161
32 Perczel, A., Hollosi, M., Tusnady, G. and Fasman, G. D. (1991) Convex constraint analysis: a natural deconvolution of circular dichroism curves of proteins. Protein Eng. **4**, 669–679
33 Philo, J. S. (1997) An improved function for fitting sedimentation velocity data for low-molecular-weight solutes. Biophys. J. **72**, 435–444
34 van Holde, K. E. (1986) Methods for the separation and characterization of macromolecules. In Physical Biochemistry, 2nd edition, pp. 110–136, Prentice-Hall, Englewood Cliffs, NJ
35 Luo, J., Iwakura, M. and Matthews, C. R. (1995) Detection of a stable intermediate in the thermal unfolding of a cysteine-free form of dihydrofolate reductase from *Escherichia coli*. Biochemistry **34**, 10669–10675
36 Park, Y. C. and Bedouelle, H. (1998) Dimeric tyrosyl-tRNA synthetase from *Bacillus stearothermophilus* unfolds through a monomeric intermediate. A quantitative analysis under equilibrium conditions. J. Biol. Chem. **273**, 18052–18059
37 Corbett, R. J. T. and Roche, R. S. (1984) Use of high-speed size-exclusion chromatography for the study of protein folding and stability. Biochemistry **23**, 1888–1894
38 Semisotnov, G. V., Rodionova, N. A., Razgulyaev, O. I., Uversky, V. N., Gripas, A. F. and Gilmashin, R. I. (1991) Study of the ''molten globule'' intermediate state in protein folding by a hydrophobic fluorescent probe. Biopolymers **31**, 119–128
39 Kotb, M., Mudd, H., Mato, J. M., Geller, A. M., Kredich, N. M., Chou, J. Y. and Cantoni, G. L. (1997) Consensus nomenclature for the mammalian methionine adenosyltransferase genes and gene products. Trends Genet. **13**, 51–52
40 Privalov, P. L. (1979) Stability of proteins: small globular proteins. Adv. Protein Chem. **33**, 167–241
41 Johnson, C. R., Morin, P. E., Arrowsmith, C. H. and Freire, E. (1995) Thermodynamic analysis of the structural stability of the tetrameric oligomerization domain of p53 tumor suppressor. Biochemistry **34**, 5309–5316
42 Mateu, M. G. and Fersht, A. R. (1998) Nine hydrophobic side chains are key determinants of the thermodynamic stability and oligomerization status of tumour suppressor p53 tetramerization domain. EMBO J. **17**, 2748–2758
43 Backman, J., Schäfer, G, Wyns, L and Bönisch, H. (1998) Thermodynamics and kinetics of unfolding of the thermostable trimeric adenylate kinase from the archaeon *Sulfolobus acidocaldarius*. J. Mol. Biol. **284**, 817–833
44 Panse, V. G., Swaminathan, C. P., Aloor, A. J., Surolia, A. and Varadarajan, R. (2000) Unfolding thermodynamics of the tetrameric chaperone, SecB. Biochemistry **39**, 2362–2369
45 Myers, J. K., Pace, C. N. and Scholtz, J. M. (1995) Denaturant *m* values and heat capacity changes: relation to changes in accessible surface areas of protein unfolding. Protein Sci. **4**, 2138–2148
46 Dignam, J. D., Qu, X. and Chaires, J. B. (2001) Equilibrium unfolding of *Bombyx mori* glycyl-tRNA synthetase. J. Biol. Chem. **276**, 4028–4037
47 Hoffman, J. L. and Kunz, G. L. (1977) Differential activation of rat liver methionine adenosyltransferase isozymes by dimethylsulfoxide. Biochem. Biophys. Res. Commun. **77**, 1231–1236
48 Kunz, G. L., Hoffman, J. L., Chia, C. S. and Stremel, B. (1980) Separation of rat liver methionine adenosyltransferase isozymes by hydrophobic chromatography. Arch. Biochem. Biophys. **202**, 565–572
49 Slavík, J. (1982) Anilinonaphthalene sulfonate as a probe of membrane composition and function. Biochim. Biophys. Acta **694**, 1–25
50 Reddy, G. B., Srinivas, V. R., Ahmad, N. and Surolia, A. (1999) Molten globule-like state of peanut lectin monomer retains its carbohydrate specificity. Implications in protein folding and legume lectin oligomerization. J. Biol. Chem. **274**, 4500–4503
51 Woody, R. W. (1995) Circular dichroism. Methods Enzymol. **246**, 34–71

Received 11 September 2001/15 October 2001; accepted 7 November 2001